Proceedings of the ASME 2011 International Mechanical Engineering Congress & Exposition
IMECE 2011
November 11-17, 2011, Denver, Colorado, USA

IMECE2011-65515

DYNAMIC BRITTLE FRACTURE CAPTURED WITH PERIDYNAMICS

Youn D. Ha
Department of Naval Architecture
Kunsan National University
Gunsan, Jeonbuk 573-701 South Korea
Email: ydha@kunsan.ac.kr

Florin Bobaru*
Department of Engineering Mechanics
University of Nebraska-Lincoln
Lincoln, Nebraska 68588-0526 USA
Email: fbobaru2@unl.edu

ABSTRACT

The bond-based peridynamic model is able to capture many of the essential characteristics of dynamic brittle fracture observed in experiments: crack branching, crack-path instability, asymmetries of crack paths, successive branching, secondary cracking at right angles from existing crack surfaces, etc. In this paper we investigate the influence of the stress waves on the crack branching angle and the velocity profile. We observe that crack branching in peridynamics evolves as the phenomenology proposed by the experimental evidence [1]: when a crack reaches a critical stage (macroscopically identified by its stress intensity factor) it splits into two or more branches, each propagating with the same speed as the parent crack, but with a much reduced process zone.

INTRODUCTION

Experiments on dynamic brittle fracture in amorphous materials exhibit a large variety complex phenomena (see [1–6]): crack branching, crack-path instability, successive branching events, secondary cracking, asymmetries of crack paths, etc. In a brittle material, cracks propagate rapidly and may curve or split into two or more branches successively. Experiments [6] also have shown that stress waves influence in a significant way the crack propagation paths and that such pulses can generate cracks propagating normal to an existing crack path. In this paper we use the peridynamic model (see [7], [8], [9]) to compute solutions to dynamic brittle fracture problems and help explain some of the characteristic features observed by experimentalists in dynamic brittle fracture events. We show that the peridynamic model supports the recent conclusions drawn from experiments (see [1]) regarding the evolution of dynamic fracture when crack branching events take place. This is the first model that is capable of relating the macroscopic behavior of a dynamically running crack and the evolution of damage at a micro-level, in this case the level of the peridynamic bonds.

Significant efforts have been dedicated to simulate dynamic brittle fracture phenomena over the past several decades. Progress has been made in the last two decades (see, e.g., [10]) but some fundamental issues and quantitative comparisons of the simulation results to experimental observations remain open (see [1]). A relatively new continuum model, peridynamics, originally designed for modeling dynamic fracture, has been introduced in [7]. Recent results obtained in [8,9] show that peridynamics correctly reproduces many of important features of dynamic crack propagation. In particular, the crack propagation speed and the crack path obtained with peridynamics appear converge [8] once the horizon reached sub-millimeter values. Also, the analysis in [9] showed that the source of a slight asymmetry of the crack path in a crack branching event, from a geometrically symmetric model, is the asymmetries of the round-off errors induced by the different order of terms in calculations of sums for nodal forces. This difference springs from the search for the neighboring nodes. We also noticed [9] that a dramatically-enhanced crack path instability and asymmetry of the branching patterns are obtained when fracture energy values that change with the local damage are used. The peridynamic model also replicated well the experimentally observed successive branching events and secondary cracking. Secondary cracks perpendicular to the

*Address all correspondence to this author.

parent cracks formed as a direct consequence of wave propagation and reflection from the boundaries [9], confirming the conclusions from experiments [6].
In this paper, we employ the bond-based peridynamic model to investigate the influence of the stress waves on the crack branching angle and the velocity profile of a propagating crack in a branching event. We observe that crack branching in peridynamics evolves as described by the phenomenology proposed by the experimental evidence [1]: when a crack reaches a critical stage (macroscopically identified by its stress intensity factor) it splits into two or more branches, each propagating with the same speed as the parent crack, but with a much reduced process zone. The results confirm the recent conclusions (see [1], [11]) that dynamic fracture in brittle materials happens through an evolution of micro-damage and micro-cracking and is controlled by the "inner problem" taking place in the process zone (see [1]) rather then by the "outer problem" that classical fracture mechanics solves.

PERIDYNAMIC FORMULATION

The peridynamic formulation [7] uses integration of pairwise forces between several material points separated by a finite distance instead of spatial derivatives in the equations of motion. Therefore, it does not face the mathematical inconsistencies that the classical formulation faces at material discontinuities. The peridynamic equations of motion at a point $\boldsymbol{x}$ and time t are:

$$\rho \ddot{\boldsymbol{u}}(\boldsymbol{x},t) = \int_{H_{\boldsymbol{x}}} \boldsymbol{f}(\boldsymbol{u}(\boldsymbol{x}',t) - \boldsymbol{u}(\boldsymbol{x},t, \boldsymbol{x}'-\boldsymbol{x})d\boldsymbol{x}') + \boldsymbol{b}(\boldsymbol{x},t), \qquad (1)$$

where $\ddot{\boldsymbol{u}}$ is the acceleration vector field, $\boldsymbol{u}$ is the displacement vector field, $\boldsymbol{b}$ is a prescribed body force intensity, and ρ is mass density. Also, $\boldsymbol{f}$ is the pairwise force function in the peridynamic bond that connects material points $\boldsymbol{x}$ and $\boldsymbol{x}'$. $H_{\boldsymbol{x}}$ is the internal subregion defined by the horizon δ.
A micro-elastic material [7] is defined when the pairwise force derives from a micro-elastic potential ω:

$$\boldsymbol{f}(\boldsymbol{\eta},\boldsymbol{\xi}) = \frac{\partial \omega(\boldsymbol{\eta},\boldsymbol{\xi})}{\partial \boldsymbol{\eta}}, \qquad (2)$$

where $\boldsymbol{\xi} = \boldsymbol{x}' - \boldsymbol{x}$ is the relative position and $\boldsymbol{\eta} = \boldsymbol{u}(\boldsymbol{x}',t) - \boldsymbol{u}(\boldsymbol{x},t)$ is the relative displacement between points $\boldsymbol{x}$ and $\boldsymbol{x}'$. A linear micro-elastic material is obtained if we take

$$\omega(\boldsymbol{\eta},\boldsymbol{\xi}) = \frac{c(\boldsymbol{\xi}) s^2 \|\boldsymbol{\xi}\|}{2} \quad where \quad s = \frac{\|\boldsymbol{\eta}+\boldsymbol{\xi}\| - \|\boldsymbol{\xi}\|}{\|\boldsymbol{\xi}\|}, \qquad (3)$$

where $c(\boldsymbol{\xi})$ is called the micromodulus function. The corresponding pairwise force is derived from Eqs. (2-3):

$$\boldsymbol{f}(\boldsymbol{\eta},\boldsymbol{\xi}) = \begin{cases} \frac{\boldsymbol{\xi}+\boldsymbol{\eta}}{\|\boldsymbol{\xi}+\boldsymbol{\eta}\|} cs, & \|\boldsymbol{\xi}\| \le \delta \\ \boldsymbol{0}, & \|\boldsymbol{\xi}\| > \delta \end{cases} \qquad (4)$$

Here we use the 2D "constant" micromodulus (see [8]) with the plane stress assumption, such as

$$c = \frac{6E}{\pi \delta^3 (1-\nu)} \qquad (5)$$

where E is the elastic Young's modulus and ν is the Poisson ratio. In the bond-based peridynamics used in this paper, the particles interact only through a pair-potential. This assumption results in an effective Poisson ratio of 1/3 in 2D plane stress and 1/4 in 3D, for an isotropic and linear micro-elastic material [12]. This limitation can be removed as shown in [7], and it does not exist in the state-based peridynamics [13].
The micromodulus computed above is obtained for material points fully inside the bulk. Because of this, the micromodulus for points near a boundary is actually underestimated. This leads to an effectively "softer" material near the boundary. We call this the peridynamic "skin effect". Obviously, as the horizon δ decreases to zero, the skin effect becomes negligible.
In peridynamics, material points are connected via elastic bonds and each bond can have a critical relative elongation, s_0 [7, 14] that models micro-damage. A bond breaks and no longer sustains force when its deformation is beyond this predefined limit s_0. Once a micro-elastic bond breaks, it stays broken. Hence the deformation of a micro-elastic material is history-dependent [14]. The critical relative elongation parameter can be obtained by matching the measured fracture energy to the energy required to completely separate a peridynamic micro-elastic body into two halves across a fracture plane, which requires breaking all the bonds that initially connected points in the opposite halves. The energy per unit fracture length in 2D (or fracture area in 3D) for the complete separation of the body into two halves is the fracture energy, G_0. In 3D, Silling and Askari [14] relate s_0 with this measurable quantity, G_0. s_0 for 2D constant micromodulus given in Eq. (5) is (see [8])

$$s_0 = \sqrt{\frac{4\pi G_0}{9E\delta}}. \qquad (6)$$

Similar to the reason for the effectively softer material near a boundary, we have an effectively "weaker" material in regions where damage already happened, or near the boundary, if we use a constant s_0 (and if the same horizon δ is used everywhere).

Therefore, a "weaker" material is in front of the crack tip than in the bulk of the material. However, if we modify s_0 to strengthen the material in zones with existing damage in an approximate way as given in Eq. (7), we observe the effects this modification has on the crack path stability and the crack propagation speed (for details of symmetry-breaking, see [9]).

$$s = \begin{cases} s_0 \times min[\gamma, 1+\beta \times \frac{D-\alpha}{1-D}] & D > \alpha \\ s_0, & otherwise \end{cases} \quad (7)$$

where the damage index D is defined as the ratio of the number of broken bonds to the number of initially bonds. Also, α, β, and γ are damage stretch coefficients: if α=β=0 and γ=1 we recover the constant s_0 model.

DYNAMIC BRITTLE FRACTURE SIMULATIONS

Problem setup

We consider a thin rectangular plate shown in Fig. 1 and a long horizontal pre-notch under remote, symmetric opening loading condition. We apply the loads suddenly and keep them constant during the dynamic simulation. This type of loading generates sharp stress waves (shock waves) that move through the material and meet along the pre-crack line. The resulting tensile stresses make the crack run and, eventually, once a sufficient stress intensity factor is reached, the running crack branches. Many experiments (see [2]) use static loading to produce dynamically running cracks in glasses. Such a loading would be too costly to attempt with an explicit code like the one used here. To eliminate the shock waves that generate the propagation from the loading mentioned above, we alternatively apply a constant velocity along the loading boundary with an initial condition for the velocity fields linearly varying from top to bottom. This condition does not generate waves (other than those produced by the running crack itself), but it is still a dynamic loading (displacement controlled) compared with the static loading (load controlled) from the experiments in [2]. All simulation results in this paper are from explicit dynamic analysis in two-dimensions.

The Velocity-Verlet algorithm, which is a more numerically stable version of central difference time integration, is employed. A uniform and stable time step size is used according to the nodal spacing [14]. The mid-point spatial integration scheme is used. The computational results are all based on uniform grids (uniform nodal spacing). In all numerical examples, the ratio between the horizon size δ and the grid spacing (the parameter m in [8, 9]) is about 4. Reasons for this particular value of m are given in [8] and are based on convergence tests for the crack path shape in crack branching problems.

The brittle material used in numerical tests is Duran 50 glass

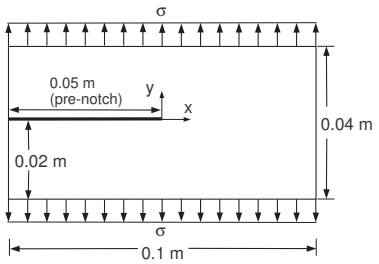

FIGURE 1. GEOMETRY AND LOADING CONDITIONS

(also used in the experiments in [15]) with density ρ=2235kg/m^3, Young's modulus E=65GPa, Poisson ratio ν=0.2, and energy release rate at branching G$_0$=204J/m^2.

Cracking branching angle and crack propagation speed

The experimental result [2] shown in Fig. 2(a) was obtained with a quasi-static loading. When the shock loading is used in the peridynamic solution, the resulting branching angle (see Fig. 3) is wider than in the experiments. To determine the reason for this, we repeat the test but this time we use the velocity boundary conditions that remove the shock wave and its reflections from the sample boundaries that propagate through the sample. The initial and boundary conditions are shown in Fig. 4. With a constant velocity of $\pm$4 m/s vertically imposed on the top and bottom boundaries (and the proper initial conditions as shown in Fig. 4) the peridynamic result is shown in Fig. 2(b). Cracks in peridynamics form as surfaces between material points as a consequence of sequential breaking of bonds. All damage maps showing the damage index D, which ultimately indicates the crack paths or diffuse damage, are using the same color-bar from red ($D > 0.4$) to blue ($D = 0$, no damage). In the absence of the stress waves, the angle of branching from the peridynamic simulation is remarkably close to that obtained from the experiments in [2]. We also compare the crack propagation speed corresponding to a crack that branches. As seen in Fig. 5, the crack propagation speed profiles for both the experiment and peridynamic simulation are very similar. In particular, the propagation speed decreases only slightly at the branching point. This is also observed in experiments (see [1,3,4,16]). We emphasize that peridynamics does not use any criterion for crack branching: this phenomenon happens as part of the solution. The only damage parameter input in the model is the relative elongation (see Eq. (6)) of an individual peridynamic bond, which is correlated to the fracture energy of the material.

The dynamic fracture phenomenon may involve one or multiple length scales (see, e.g. [17]). Dynamic cracks in brittle materials appear to grow via a mechanism of damage spreading through

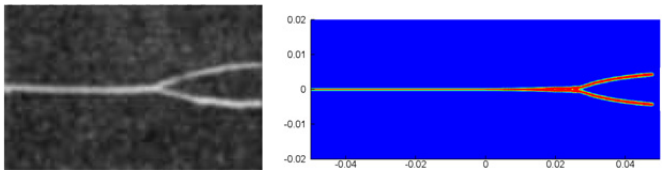

(a) Experimental crack path [2] (b) Peridynamic crack path

FIGURE 2. CRACK BRANCHING PATH: EXPERIMENT VS. PERIDYNAMICS

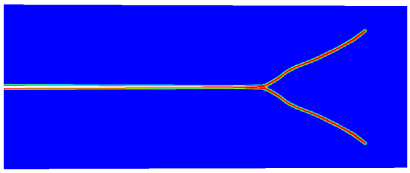

FIGURE 3. PERIDYNAMIC DAMAGE MAP FOR THE BRANCHING CRACK WITH SHOCK LOADING

the nucleation and growth of microcracks (see [11]). A better understanding of the relationship between the dynamics of propagation of both the microcracks and the macroscopic crack is still needed, as mentioned in [11]. Material microstructure is likely to play an important role in this respect. The peridynamic models in the present work are for an ideal homogeneous material. The results with such homogeneous materials in [8] indicate that we have δ-convergence in the dynamic crack branching problem (as the nonlocal region decreases, the propagation speed reaches stable values). Interestingly, the peridynamic results for the crack propagation speed in soda-lime glass (density ρ=2440kg/m^3, Young's modulus E=72GPa, Poisson ratio ν=0.22, and energy release rate at branching G_0=135J/m^2 from [2]) are close, or even slightly higher, than those obtained for Duran glass. Experiments with static loading showed a lower propagation velocity in soda-lime glass than in Duran glass. This discrepancy could be an indication that the connection, suggested by experiments, between the dynamics of the microcracks and that of the macrocracks, which may be material-dependent, has to be inserted somehow into the peridynamic model. Presently, the dynamics of the macrocrack in a peridynamic model is completely determined by the dynamics of the micro-damage of the peridynamic bonds, and the loading conditions. Taking into account microstructural difference that can lead to differences in the dynamics of micro-cracks growth between two materials is subject of future research.

Evolution of crack branching

After decades of careful experiments, a certain phenomenology for the crack branching process in brittle amorphous materials has crystalized [1]: when a crack reaches a critical stage (macroscopically identified by its stress intensity factor) it splits into two or more branches, each propagating with the same speed as the parent crack, but with a much reduced *process zone*. The conclusion drawn from experiments ([1], [11]) is that dynamic fracture in brittle materials happens through an evolution of micro-damage and micro-cracking and is controlled by the "inner problem" taking place in the process zone ([1]) rather then by the "outer problem" that classical fracture mechanics solves. This explains the discrepancies between the results produced by the linear fracture mechanics theory and by the experiments. Here we analyze the peridynamic results for crack branching and observe that crack branching in peridynamics evolves as deduced from the experiments. Indeed, from Fig. 6 we notice that before branching occurs, the damage zone of the single propagating crack thickens and once branching occurs the "process zone" reduces significantly. This happens without much change in the propagation speed. In order to show clearer the crack thickening process prior to branching and the reduction of the process zone after branching, in Fig. 6 we use the legend for the damage from 0 to 1. Notice again that the damage legend is 0 to 0.45 for all other peridynamic damage maps shown in this paper.

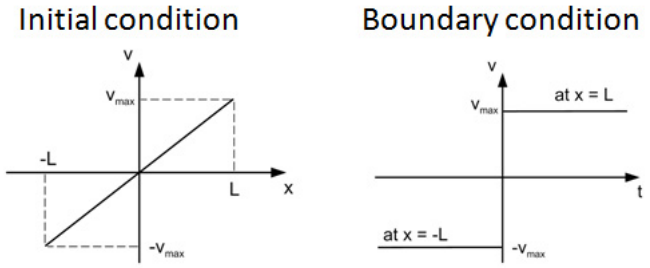

FIGURE 4. VELOCITY BOUNDARY AND INITIAL CONDITIONS

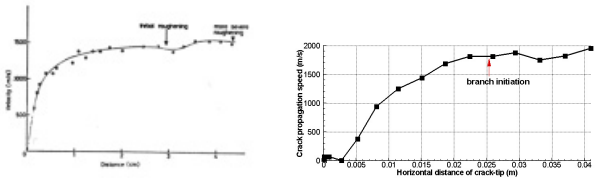

(a) Experimental crack speed [16] (b) Peridynamic crack speed

FIGURE 5. CRACK PROPAGATION SPEED: EXPERIMENT VS. PERIDYNAMICS

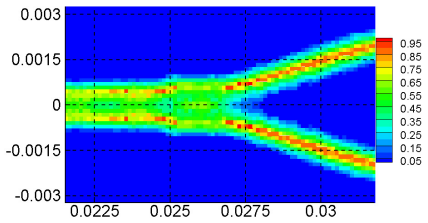

FIGURE 6. CLOSE-UP DAMAGE ZONE AROUND BRANCH POINT OF FIG. 2(b)

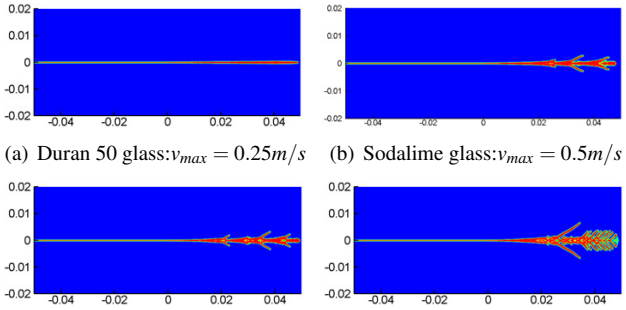

(a) Duran 50 glass:$v_{max} = 0.25m/s$ (b) Sodalime glass:$v_{max} = 0.5m/s$

(c) Duran 50 glass:$v_{max} = 0.75m/s$ (d) Sodalime glass:$v_{max} = 1.0m/s$

FIGURE 7. PERIDYNAMIC RESULTS: VARIOUS FRACTURE PATTERNS IN DIFFERENT MATERIALS

Arrested branching and influence of the material properties

It is interesting to notice that a crack arrest criterion is not required in peridynamics. With the velocity-imposed boundary conditions, Fig.7 show the damage map for a propagating crack that has several attempts to branch, yet none is successful and the parent crack continues to grow. This behavior is controlled by the loading conditions: faster motion induces multiple attempts at branching, while slower motion may result in no branching, or a single successful branching event (see Fig. 7). Notice that the peridynamic models produce similar patterns of fracture in both soda-lime and Duran glass as long as the loading is higher for Duran glass (see Fig.7 and Fig. 8). Cascade branching (see Fig. 9) is easier to obtain using the shock loading, while the dynamic displacement-controlled conditions with a linear initial velocity profile from top to bottom gives rise to "fish-bone"-like multiple branching attempts when the loading is increased past a certain value.

CONCLUSIONS

Simulating dynamic brittle fracture in amorphous materials is an open problem. The results presented here demonstrate the capabilities of peridynamic models in capturing essential features of dynamics fracture. We have shown that stress waves

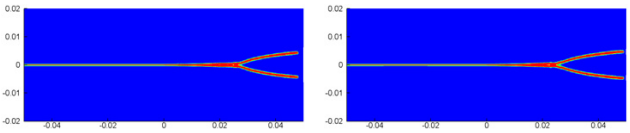

(a) Duran 50 glass:$v_{max} = 0.5m/s$ (b) Sodalime glass:$v_{max} = 0.4m/s$

FIGURE 8. PERIDYNAMIC RESULTS: SIMILAR BRANCHING PATTERNS IN DIFFERENT MATERIALS

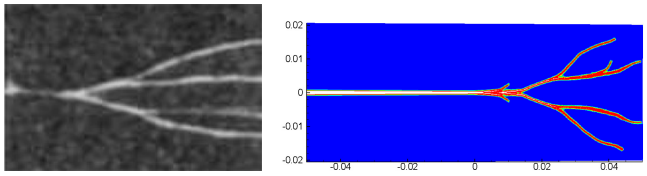

(a) Experimental crack path [4] (b) Peridynamic crack path

FIGURE 9. SUCCESSIVE BRANCHING: EXPERIMENT VS. PERIDYNAMICS

influence the crack branching angle and the velocity profile. We also observed that crack branching in peridynamics evolves in a similar way with the phenomenology proposed by the experimental evidence: when a crack reaches a critical stage (macroscopically identified by its stress intensity factor) it splits into two or more branches, each propagating with the same speed as the parent crack, but with a much reduced process zone. For a particular material, connecting the dynamics of the micro-cracking nucleation and growth with that of the macrocracks appears to be the next step in developing a fully predictive model for dynamic brittle fracture.

ACKNOWLEDGMENT

This work has been supported by grants from the Sandia National Laboratories (project manager Dr. S.A. Silling) and the Boeing Co. (project manager Dr. E. Askari). We thank to Dr. Silling, Dr. Askari and Dr. M.L. Parks (Sandia) for very useful discussions.

REFERENCES

[1] Ravi-Chandar, K., 2004. *Dynamic Fracture*. Elsevier.

[2] Bowden, F., Brunton, J., Field, J., and Heyes, A., 1967. "Controlled fracture of brittle solids and interruption of electrical current". *Nature,* ***216***, pp. 38–42.

[3] Ramulu, M., and Kobayashi, A. S., 1985. "Mechanics of crack curving and branching a dynamic fracture analysis". *International Journal of Fracture,* ***27***(3), pp. 187–201.

[4] Ramulu, M., Kobayashi, A., Kang, B., and Barker, D.,

1983. "Further studies on dynamic crack branching". *Experimental Mechanics,* ***23***(4), pp. 431–437.

[5] Ravi-Chandar, K., and Knauss, W., 1984. "An experimental investigation into dynamic fracture: Iii. on steady-state crack propagation and crack branching". *International Journal of Fracture,* ***26***(2), pp. 141–154.

[6] Ravi-Chandar, K., and Knauss, W., 1984. "An experimental investigation into dynamic fracture: Iv. on the interaction of stress waves with propagating cracks". *International Journal of Fracture,* ***26***(3), pp. 189–200.

[7] Silling, S., 2000. "Reformulation of elasticity theory for discontinuities and long-range forces". *Journal of the Mechanics and Physics of Solids,* ***48***(1), pp. 175–209.

[8] Ha, Y., and Bobaru, F., 2010. "Studies of dynamic crack propagation and crack branching with peridynamics". *International Journal of Fracture,* ***162***(1), pp. 229–244.

[9] Ha, Y., and Bobaru, F., 2011. "Characteristics of dynamic brittle fracture captured with peridynamics". *Engineering Fracture Mechanics,* ***78***(6), pp. 1156–1168.

[10] Belytschko, T., Chen, H., Xu, J., and Zi, G., 2003. "Dynamic crack propagation based on loss of hyperbolicity and a new discontinuous enrichment". *International Journal for Numerical Methods in Engineering,* ***58***(12), pp. 1873–1905.

[11] Scheibert, J., Guerra, C., Célarié, F., Dalmas, D., and Bonamy, D., 2010. "Brittle-quasibrittle transition in dynamic fracture: An energetic signature". *Phys. Rev. Lett.,* ***104***(4), Jan, p. 045501.

[12] Gerstle, W., Sau, N., and Silling, S., 2007. "Peridynamic modeling of concrete structures". *Nuclear Engineering and Design,* ***237***(12-13), pp. 1250–1258.

[13] Silling, S., Epton, M., Weckner, O., Xu, J., and Askari, E., 2007. "Peridynamic states and constitutive modeling". *Journal of Elasticity,* ***88***(2), pp. 151–184.

[14] Silling, S., and Askari, E., 2005. "A meshfree method based on the peridynamic model of solid mechanics". *Computers and Structures,* ***83***(17-18), pp. 1526–1535.

[15] Doll, W., 1975. "Investigations of the crack branching energy". *International Journal of Fracture,* ***11***(1), pp. 184–186.

[16] Field, J., 1971. "Brittle fracture: its study and application". *Contemporary Physics,* ***12***(1), pp. 1–31.

[17] Livne, A., Ben-David, O., and Fineberg, J., 2007. "Oscillations in rapid fracture". *Physical Review Letters,* ***98***(12), p. 124301.